# Modelling the growth potential of the kelp *Saccharina latissima* in the North Atlantic

**Jago Strong-Wright** [1], **John R. Taylor** [2,3,*]

[1] *St. John's College, Cambridge and University of Cambridge*
[2] *Department of Applied Mathematics and Theoretical Physics, University of Cambridge*
[3] *Centre for Climate Repair at Cambridge*

Correspondence*:
John R. Taylor
J.R.Taylor@damtp.cam.ac.uk

## ABSTRACT

It has recently been proposed that macroalgae (e.g. kelp) could be grown in the open ocean as a $CO_2$ removal strategy. Most macroalgae naturally grow in shallow coastal waters, and their ability to grow in open ocean conditions is largely untested. Here we quantify macroalgae growth potential in the North Atlantic using an established model of *Saccharina latissima* forced by an ocean state estimate. In the relatively clear open ocean waters, we find that growth is possible to depths of up to 50m across most of the region, with higher growth between 40°N and 50°N. The model exhibits a large carbon to nitrogen ratio at the southern end of the growth range. The ratio of kelp carbon to phytoplankton biomass is also relatively high in the southeastern portion of the growth range. Using a sensitivity analysis, we find that the position of the southern limit of the growth range is largely modulated by temperature tolerance on the western side of the basin in the Gulf Stream and low nitrates on the eastern side of the basin. We also find a statistically significant reduction in the kelp growth potential over the period from 2002-2019, reflecting the warming of the surface ocean over this period.

**Keywords: seaweed, macroalgae, kelp, modelling, carbon**

## 1 INTRODUCTION

There is an urgent need for carbon dioxide removal (CDR) strategies to be developed in order to limit the warming of global mean surface air temperature to less than $2°C$ by 2100 (Lee et al., 2021). In order to meet this target, negative net $CO_2$ emissions are required by 2050 (Rogelj et al., 2018). The biological sink of carbon in the North Atlantic, by which carbon dioxide is stored largely through photosynthesis, removes between $4$ and $18\%$ of annual anthropogenic carbon dioxide emissions (Sanders et al., 2014; Canadell et al., 2021). There are several methods that have been explored to enhance this sink such as iron fertilisation and artificial up-welling (Canadell et al., 2021).

One method that has been proposed is the growth of macroalgae on artificial substrates in the open ocean, away from their native habitat (rocky bottomed coastal waters). For example, Whiting et al. (2020) modeled kelp growth on free-floating platforms off the West Coast of the United States. Using a coupled hydrodynamic-biogeocheical-kelp model for *Saccharina latissima* (*S. latissima*), Broch et al. (2019) found that the offshore waters were more suitable for kelp growth than the coastal waters off the coast of Norway.

However, the ability of macroalgae to grow in broader open ocean conditions remains largely untested. Here, we quantify the growth potential for *S. latissima* in the North Atlantic ocean, using an established kelp growth model (Broch and Slagstad, 2012; Broch et al., 2013) forced with output from an ocean state estimate (E.U. Copernicus Marine Service Information, 2021a,d,b,c).

Our primary objectives are to uncover the spatial patterns associated with kelp growth in the open ocean and to quantify the carbon and nitrogen stored within the fronds at the end of a single growing season. This could help identify target regions for future field trials. It is important to note that we do not attempt to capture the influence of macroalgae on phytoplankton or other components of the biogeochemical system, and thus we do not quantify the carbon sequestration potential of this strategy. Nevertheless, modelling the kelp growth potential in the open ocean is a useful first step and we hope that it leads to future work to quantify the carbon sequestration potential using fully coupled hydrodynamic-biogeochemistry-kelp models and field measurements.

Below, in section 2 we describe the configuration and forcing of the growth model for *S. latissima*. In section 3, we describe the geographical and vertical distribution of kelp biomass and the seasonal growth patterns and calculate the carbon:nitrogen ratio at the end of the growth period. The latter is important because nitrates that are consumed by the kelp could have been used by phytoplankton and hence uptake of nitrates by the kelp could reduce primary production in a coupled system. We also examine the sensitivity of the results to a few key parameters. Finally, we end in section 4 with a discussion of the results and the implications for future work.

## 2 METHODS

### 2.1 Model

Here, we use a growth model for *S. latissima* (sugar kelp) first proposed by Broch and Slagstad (2012). This species was chosen because it is relatively well-studied due to its widespread use in aquaculture and it has been proposed as a candidate for offshore macroalgae farms (Broch et al., 2019; Whiting et al., 2020; Running Tide, 2021). Although other models for *S. latissima* have been developed (e.g. Venolia et al., 2020), we use the model first described in Broch and Slagstad (2012) because it has been tested in North Atlantic conditions (Broch and Slagstad, 2012; Broch et al., 2013; Molen et al., 2018; Broch et al., 2019) and its inputs (temperature, nitrate concentration, and irradiance) are readily available from ocean state estimates and reanalysis products.

The kelp growth model consists of three coupled ordinary differential equations governing the evolution of the three primary state variables; frond area ($A$), nitrogen reserves ($N$) and carbon reserves ($C$). We followed the implementation described in Broch and Slagstad (2012) with the modifications later proposed in Broch et al. (2013), except that we use a more accurate and efficient fourth order Runge-Kutta scheme instead of the explicit Euler scheme used in Broch and Slagstad (2012). We validated the model by repeating the experiments reported in Broch and Slagstad (2012). Our implementation of the model has been made publicly available (Strong-Wright, 2021) in the Julia programming language. The reader is referred to the description of the code and Broch and Slagstad (2012); Broch et al. (2013) for details of the implementation.

The kelp growth model was forced using temperature and nitrate concentrations from the Mercator Ocean physics and biogeochemical analysis and reanalysis (E.U. Copernicus Marine Service Information, 2021a,d,b,c), and the photosynthetically available radiation (PAR) was obtained from NASA's Joint Polar

Satellite system and Moderate-resolution Imaging Spectroradiometer (NASA Goddard Space Flight Center, Ocean Ecology Laboratory, Ocean Biology Processing Group, 2021b,a). The diffuse attenuation coefficient was derived from the chlorophyll concentration using the method described by Morel (1988) and modified by Morel and Maritorena (2001) (the same method used in the biogeochemical model; Aumont et al. (2015)). The temperature was available at 1/12° resolution but this was sub-sampled at the 1/4° resolution of the biogeochemical model to force the kelp growth model. The PAR was available at 9km resolution and was also subsampled at 1/4° resolution. Missing PAR values due to cloud cover or low light levels were filled in using linear interpolation.

The initial conditions for the state variables match the values used in Broch and Slagstad (2012), specifically $A = 0.1\text{dm}^2$, $N = 0.022\text{gN(g sw)}^{-1}$, and $C = 0.3\text{gC(g sw)}^{-1}$. The sensitivity of the results to these initial conditions was evaluated by varying the initial conditions with constant forcing conditions (see Supplementary Material). This analysis revealed that for sufficiently small initial area, the model results are not very sensitive to the initial carbon and nitrogen reserves. Further, the analysis showed that for a large range of initial areas, all runs converged to the same equilibrium state with constant forcing. These results are shown in Figures S1 and S2 of the Supplementary Material.

After validation and testing, the kelp growth model was applied to a static grid over the area between $0$ and $80°$W, and $35$ and $65°$N. The depth range $0$ to $75$m was used since we found no significant growth below this depth range. In the baseline runs a $1/4°$ grid with 2m depth resolution was used, and for parameter variation analysis a $1°$ grid with the same depth resolution was used.

For the simulations shown the main text we run the model from December $1^{\text{st}}$ to January $4^{\text{th}}$ two calendar years later (i.e. for a period of 400 days). This time frame was chosen for several reasons: Start dates around this time yield very similar results (variation in the temporal change of conditions over a small range is captured in the ensemble described below), and by the end date the maximum total carbon of the run has been surpassed. Figure S3 in the Supplementary Material shows the total carbon for various start dates. Unless otherwise noted, the model is run from the end of 2019 (01/12/2019) until the start of 2021 (04/01/2021).

We do not consider self-shading or nutrient uptake by the kelp. This is likely to be a reasonable assumption for the purposes of estimating the kelp growth if the density of the kelp is sufficiently low. After scaling our model results such that there is one vertical line of kelp in each square kilometer of ocean and with 100 kelp fronds per meter in the vertical, the total nitrate uptake by the kelp was less than $1/500$ of the nitrate uptake by phytoplankton in the same area (Louanchi and Najjar, 2001). However, there is a clear need for future work to consider a fully coupled biogeochemical model in order to assess the ecosystem impacts of offshore kelp growth and the carbon sequestration potential.

## 3 RESULTS

Figure 1(a) shows the carbon content per kelp frond, averaged in depth between 0 and 75m on the day that the depth and area-integrated carbon is maximised. The contour line in all panels shows the location where the average carbon content is equal to 5gC/frond. The kelp grows well across most of the North Atlantic with a sharp decline south of about $40°$N. The maximum carbon content generally occurs near the southern end of the growth range, between $40°$N and $45°$N with notably high values in the southeast corner of the growth range. Figure 1(b) shows the depth-averaged nitrogen content per frond on the same day. The nitrogen content shows a notably distinct pattern compared to carbon with larger values at higher latitudes.

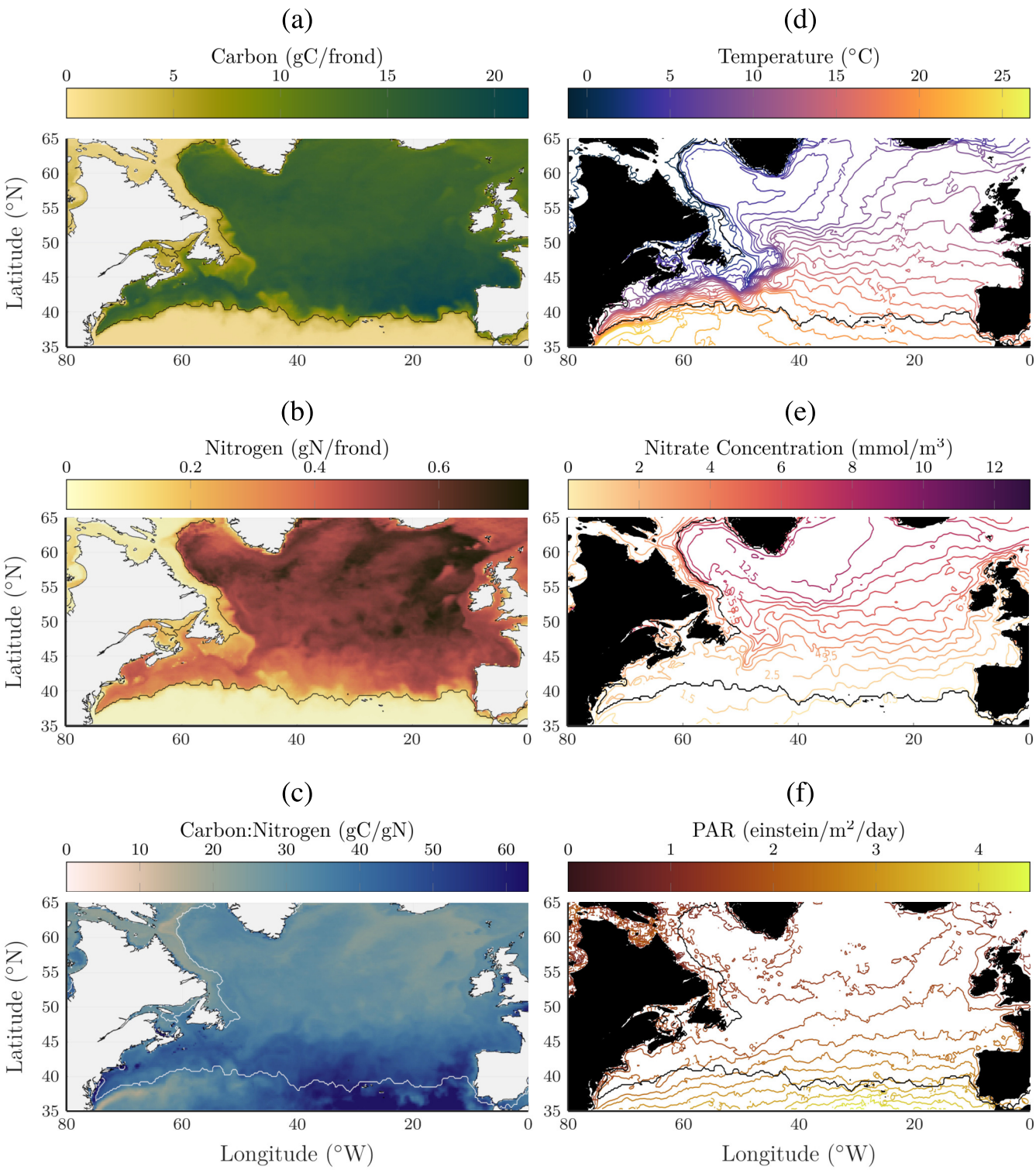


**Figure 1.** Panels A-C: depth-averaged carbon (A), nitrogen (B) and carbon:nitrogen ratio (C) on the day 344 in early November when the total carbon content is maximum in the kelp model. Panels D-F: temperature (D) and nitrate concentration (E) and photosynthetically available radiation (F) that were used as input to the kelp growth model, here shown averaged in time (400 days) and depth (0-75m) over the kelp deployment. For reference the 5gC/frond contour is shown in black (white in panel C), indicating the limits of the region with significant kelp growth.

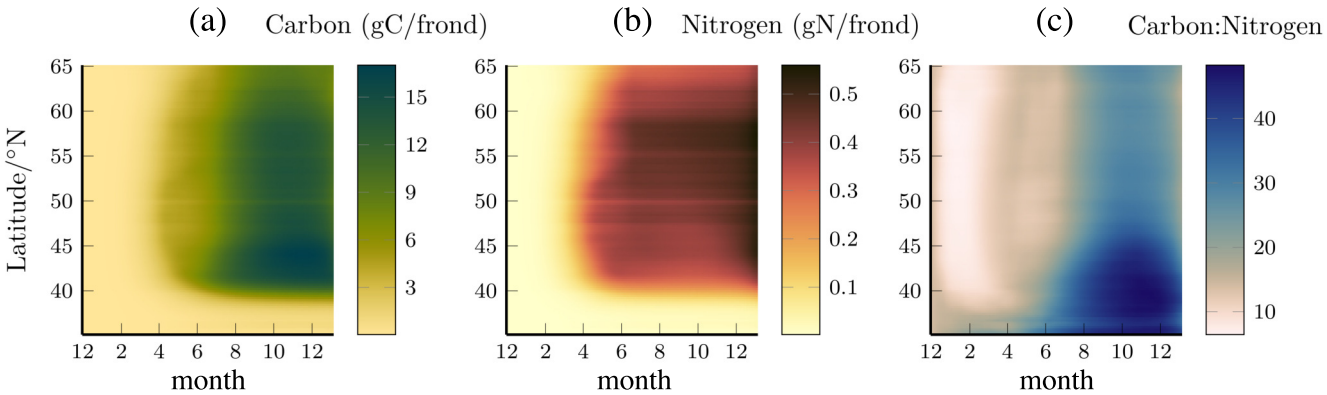


**Figure 2.** Longitude (0°W to 80°W) and depth averaged (0 to 65m) Carbon (panel A), Nitrogen (panel B), and carbon:nitrogen ratio per frond (gC/gN), as a function of time and latitude (panel C).

Figure 1(c) shows the corresponding kelp carbon:nitrogen (C:N) ratio. This ratio varies significantly across the region and reaches high values, in excess of 50 gC/gN near the southern end of the growth range (indicated in a white contour line). Note that the ratio is not meaningful south of the growth range where the carbon and nitrogen contents are small. The modeled C:N ratio is generally consistent with measurements made for kelp growing in coastal waters (22 to 32; Fossberg et al. (2018), 15 to 42; Nielsen et al. (2014), 23 to 131; Nielsen et al. (2016)).

To visualize the conditions that drive these patterns, Figure 1(d-f) shows ocean temperature, nitrate concentration, and PAR, averaged in depth and time to span the full kelp deployment. For reference, the southern end of the growth range is shown as in panels (a-c). In the kelp growth model, the maximum growth rates occur for temperatures between 10-15°C. Interestingly, the largest carbon content occurs in locations that are on average warmer than 15°C. As will be discussed below, the kelp exhibit non-trivial depth and seasonal variations which likely explain the lack of a direct link between mean temperature and kelp growth. This illustrates the utility of a dynamic kelp model that is capable of responding to time-varying local conditions.

On the western side of the North Atlantic basin, the 5gC/frond contour closely tracks the average temperature contours between 19-21°C, following the mean path of the Gulf Stream. On the eastern side of the basin, the 5gC/frond contour appears to more closely follow an average nitrate concentration of 0.5 mm/m$^3$. This, together with the observation that the C:N ratio is higher on the eastern side of the basin, suggests that kelp on the southwestern end of the growth range is primarily limited by temperature, while growth on the southeastern end of the growth range is primarily limited by nitrate. On the western side of the Labrador Sea, the 5gC/frond contour closely follows the 2°C average temperature contour. West of this contour, kelp growth is inhibited in the cold waters carried south by the Labrador Current.

Figure 2(a,b) shows the carbon and nitrogen content per frond, averaged in depth and longitude, and plotted as a function of latitude and time, and panel (c) shows the ratio of these quantities. The nitrogen content increases between April and June with the southern latitudes increasing earlier in the year. The carbon content rapidly increases in April but then plateaus before increasing again from June-August. The increase in carbon in the summer months draws down the nitrogen reserves that had been built up earlier, leading to an increase in the C:N ratio, particularly in the southern region where the ambient nitrate concentration is low and the kelp deplete their nitrogen reserves.

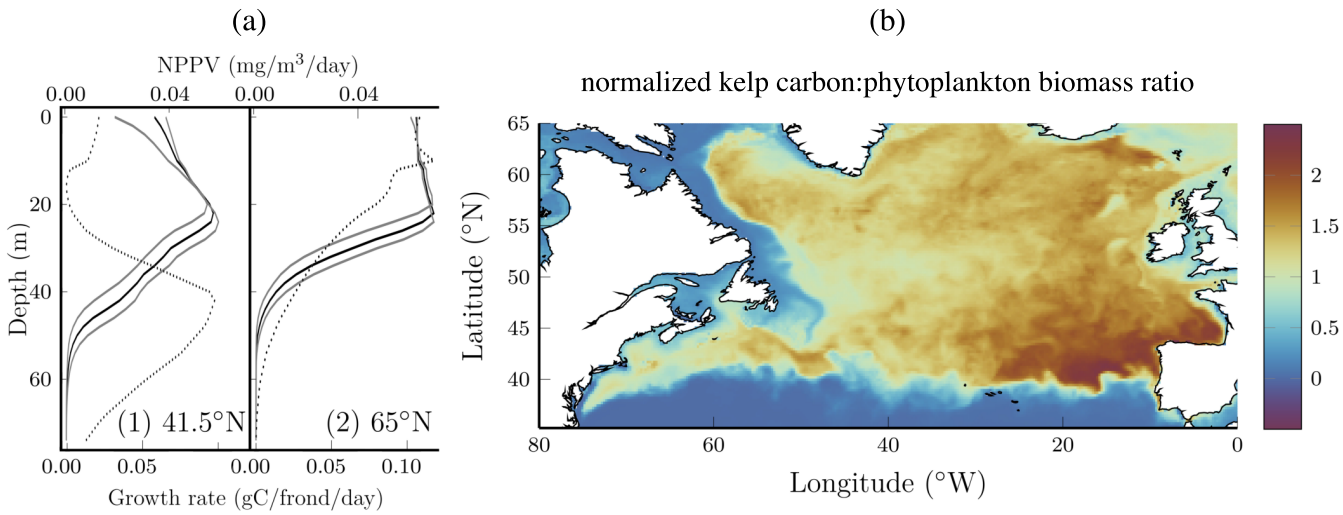


**Figure 3.** Panel (a): longitude average (0°W to 80°W) kelp growth rate (solid) at two representative latitudes on at the end of July. The depth of maximum growth rate is proportional to the photosynthetic efficiency as shown by the grey boundaries where the photosynthetic efficiency is varied by $\pm 25\%$. Panel (b): ratio of the normalised kelp carbon content to the phytoplankton biomass. Each quantity is normalized by the area average such that the ratio is unitless and if the kelp carbon and phytoplankton biomass were uniformly distributed the ratio would be 1.

The vertical distribution of kelp also changes with latitude. The solid black curves in Figure 3(a) show vertical profiles of the growth rate (measured in terms of carbon accumulation) averaged over all longitudes for two latitudes. Solid grey curves show the sensitivity to the photosynthetic efficiency which will be discussed below. For comparison, the dotted curves show the net primary production per volume (NPPV) for phytoplankton at the same locations. At 41.5N, both curves exhibit a distinct subsurface maximum which is characteristic of nutrient limitation (e.g. Yang et al., 2021), but the peak in phytoplankton NPPV is significantly deeper than the peak in the kelp growth rate, despite the fact that the kelp and phytoplankton are exposed to the same nitrate and PAR profiles. Increasing the photosynthetic efficiency deepens the subsurface maximum for kelp (lower grey curve) which suggests that differences in the response to low light conditions might explain the different depth of the subsurface maximum for phytoplankton and kelp. It should also be noted that phytoplankton are subject to advection and diffusion while kelp are not in our model.

At 65°N (Figure 3(a), right panel), the subsurface maximum for kelp and phytoplankton is less distinct and the curves are nearly constant at shallow depths. Interestingly, at this latitude the kelp growth rate remains high to a lower depth compared to the phytoplankton primary production. The reasons for this aren't immediately clear, but we speculate that this might be due to the fact that kelp in our model aren't subject to deep vertical mixing that limits phytoplankton growth at high latitudes, particularly in the winter.

Although our kelp growth model is not coupled with the biogeochemical model, it is of interest to compare the geographical distribution of kelp and phytoplankton growth. Figure 3(b) shows the ratio of normalized kelp carbon content and phytoplankton biomass. Each quantity has been normalized by the area average such that if the distribution of kelp and phytoplankton were uniform, the ratio would be 1. Interestingly, kelp grows comparatively better in the open ocean compared to the coastal waters that form their natural habitat. This can be explained by strong light attenuation in coastal waters. Together with the results shown above, this demonstrates significant growth potential for kelp in the open ocean. Within the open ocean the ratio is maximum in the southeastern region where the nitrate concentrations are relatively

low (see Fig. 1b) and highly seasonally dependent. The ability of kelp to store nitrogen in the spring and use these reserves for growth later in the year (see Fig. 2) confers an advantage over phytoplankton in regions where the nitrate concentration becomes low and is seasonally variable.

## 3.1 Sensitivity

The results above were produced with a kelp growth model with the parameters reported in Broch and Slagstad (2012) and Broch et al. (2013). We performed a sensitivity analysis to quantify the dependence on several key parameters and the initial conditions. Estimates of the photosynthetic rates for *S. latissima* vary considerably (Luning, 1979; Bartsch et al., 2008; Broch and Slagstad, 2012). To explore the sensitivity of the results to the photosynthetic rate, we varied the photosynthetic efficiency, $\alpha$, by $\pm 25\%$ about its baseline value. Varying $\alpha$ changed the depth average carbon content at all locations, primarily by changing the depth range over which kelp can grow. The grey curves in Figure 3(a) show this effect.

There is also significant uncertainty in the literature as to the maximum temperature at which *S. latissima* can grow. For example, it has been reported that there is a risk of death with no subsequent continuation of growth in water with temperatures as low as $17°$C (Gerard and Du Bois, 1988) and that consistent growth could be possible up to $22°$C (Bolton and Lüning, 1982). In the Broch and Slagstad (2012) model the growth rate includes a term that is a piecewise linear function of temperature such that the growth rate is zero for temperatures warmer than an upper limit, $T_h$. To examine the sensitivity of the results to the maximum temperature, we varied $T_h$ by $\pm 2°$C about the baseline value of $T_h = 19°$C. Varying $T_h$ shifted the position of the southern boundary of the kelp growth range (i.e. the southern contour shown in Figure 1). When $T_h$ increased, the growth boundary shifted to the south most prominently on the western side of the basin where temperature is the main limiting factor. When $T_h$ was reduced the growth boundary shifted to the north at all longitudes. It will be important to refine the estimates of the temperature tolerance of *S. latissima* if the region just north of the southern growth boundary with large carbon content and large C:N ratio is to be targeted for offshore kelp growth.

In addition to the model parameters, the kelp growth depends on the environmental conditions in a given year. To explore this dependence and the interannual variability, the model was run with data from 2002 to 2017 (i.e. runs started on 01/12/2002-2017 and ended 04/01/2004-2019). To sample the variability associated with all of these combined effects, a random ensemble of 300 runs was constructed where the photosynthetic efficiency and maximum temperature tolerance were normally distributed with standard deviations half the range given above, the year was uniformly distributed. An Analysis of Variance (ANOVA) was also performed on the ensemble and the full results of this analysis are reported in Table S1 in the Supplementary Material. Regressions showed that the relationship between the total kelp carbon growth and the phytosynthetic efficiency, and the maximum temperature tolerance is positive.

Figure 4 shows the maximum total carbon for each run in the ensemble as a function of starting year. The total carbon is normalized based on a density of 1 vertical line of kelp per km$^2$, with 100 fronds per meter in the vertical direction. Since the kelp is not coupled with the biogeochemical model, the results can be scaled to other densities with the important caveat that at high densities the kelp could significantly influence the biogeochemical system (e.g. by modifying the light levels or depleting nitrate concentrations), thereby changing the results.

The total carbon exhibits a statistically significant negative trend over the period considered (2002-2019), as shown in a linear fit in the top panel of Figure 4. The interannual variability and the linear trend in the total carbon are inversely related to the mean temperature between $35 - 45°$N (bottom panel of Figure 4). Indeed, a t-test demonstrates a strong negative correlation between these quantities ($p < 10^{-29}$). In

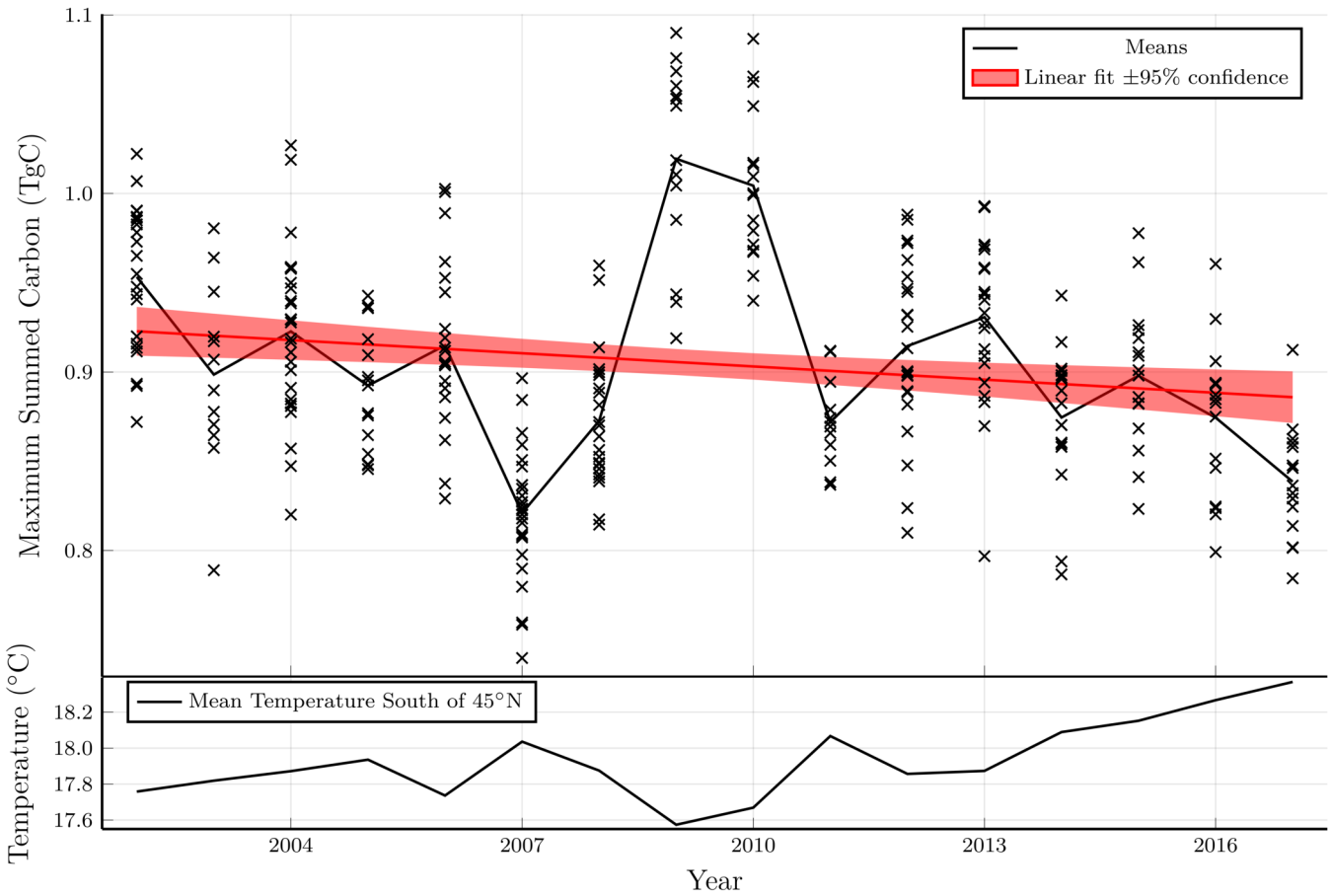


**Figure 4.** Top panel: Maximum total carbon of each model run from an ensemble with varying parameters plotted as a function of the model starting year. A linear fit to the model ensemble and a shaded region indicating the 95% confidence interval of the fit coefficients indicates a statistically significant downward trend. Bottom panel: Mean temperature averaged from 0 to 75m in depth, 0°W to 80°W in longitude and 35°N to 45°N in latitude.

years when the temperature is anomalously high, the area that is viable for kelp growth shrinks leading to a reduction in the total carbon. As discussed below, the reduction in growth potential with increasing temperatures has important implications in the presence of climate change.

## 4 DISCUSSION

Here, we used an existing model for *S. latissima* forced with reanalysis data and found that ocean conditions are favorable for kelp growth across most of the North Atlantic in a region bounded by extreme temperatures and low nitrate levels. A sensitivity study indicated that the geographical range that is favorable for growth depends on parameters in the kelp growth model and annually-varying ocean temperatures. Another notable result is the significant variability in the kelp carbon:nitrogen (C:N) ratio, with high values in regions where nitrate levels are low in the summer.

In the western side of the North Atlantic basin, the boundary of the growth region appears to be controlled by temperature constraints on kelp growth. Although the kelp growth model is forced with fields that vary in time and space, the southern growth boundary on the western side of the basin closely follows the 19-20°C annual and depth-averaged temperature contour. This is close to the maximum temperature for kelp growth

in the model which is $19°$C. Conversely, in the Labrador Sea the northern growth boundary closely follows the $2°$C contour and the path of the Labrador Current. This provides a useful way to estimate the growth range, although as noted above and discussed in the Supplementary Material, the bounding temperatures are sensitive to the model parameters. The upper temperature limit is particularly uncertain with various estimates in the literature (e.g. Bolton and Lüning, 1982; Gerard and Du Bois, 1988) and this significantly influences the size of the growth region.

On the eastern side of the basin, the growth boundary follows contours of the mean nitrate concentration (between $0.2$ and $0.5$mmol/m$^3$), implying a nitrate limitation in this area. This is consistent with observed minimum nitrate concentration limits of *S. latissima* with a significant drop in growth rate below $0.4$mmol/m$^3$;Jevne et al. (2020). Our results are consistent with the surveys reported in (Breeman, 1988) and van Den Hoek (1982) who discussed the role of temperature in controlling the growth range of various species of seaweed in coastal waters. However, while these studies considered only temperature control on the distribution, we find that low nitrate concentrations dictate the southern growth boundary in the eastern half of the North Atlantic basin.

In the southeastern part of the growth range (between the Azores and the Bay of Biscay), the modeled kelp C:N ratio at the end of the growing season is very high and kelp grow better relative to their average growth compared to phytoplankton. In these waters with low and seasonally variable nitrate concentration, the ability of kelp to store nitrogen (Sjøtun, 1993; Nielsen et al., 2014) appears to be very important. The kelp nitrogen reserves increase in the spring when nitrate concentrations are relatively high, and the nitrogen reserve is then used to fuel growth in later months.

The model indicates kelp growth to depths of about 50m in offshore conditions with a mean maximum growth rate at a depth just below 20m. For depths shallower than 20m, the mean growth rate is largely independent of photosynthetic efficiency, implying that the growth is not light limited. There are instances in very clear water where *S. latissima* has been observed at similar depths; for example Krause-Jensen et al. (2019) observed growth deeper than $61$m. However, this is significantly different to most coastal observations with a median maximum depth of $17.7$m (Krause-Jensen et al., 2019), light attenuation is much stronger.

We tested the sensitivity of the results to key parameters and environmental conditions using an ensemble of 300 model runs. A key takeaway from the ensemble was the strong negative correlation between average temperature near the southern boundary and the total kelp carbon. This raises the possibility that in the future the viable area for kelp growth will be reduced as the North Atlantic warms (Kwiatkowski et al., 2020). In the low temperature limited regions the area could be expanded as sea temperature increases, although this region is currently small. As sea ice recedes, the viable area might be extended to the north (Krause-Jensen et al., 2019). Another possible impact of the changing climate is the projected reduction in nitrate concentration, which would further decrease the viable area (Kwiatkowski et al., 2020).

The model exhibits significant geographical variability in the kelp C:N ratio across the North Atlantic. The range in the modeled C:N mass ratio is generally consistent with coastal observations of *S. latissima* (e.g. $22$ to $32$, $15$ to $42$, $23$ to $131$ Fossberg et al., 2018; Nielsen et al., 2014, 2016). The high modeled C:N ratio in the southeastern portion of the growth range can be explained by favorable light and temperature levels but low nitrate levels in these waters. The average molar ratio for kelp from our model is $31.1 \pm 0.5$ which is significantly higher than the canonical Redfield ratio of 6.6 Redfield (1934). This suggests that kelp could represent a nitrogen-efficient sink of carbon.

There are several important caveats that are worth noting. First, the kelp model assumes that nitrate is the only limiting nutrient. *S. latissima* is known to uptake ammonium (Ahn et al., 1998) and other nutrients such as phosphorus, iron, or other trace metals could limit kelp growth, particularly in the open ocean (Lubsch and Timmermans, 2019; Venolia et al., 2020; Broch et al., 2019). Offshore conditions could also expose the kelp to enhanced erosion due to strong wind and wave-generated currents. However, as noted by Broch and Slagstad (2012), there is little available information about the influence of water movement on frond erosion and this is not explicitly included in the model. Future work based on laboratory experiments or field trials could provide valuable information on these additional processes.

Here our focus was quantifying the growth potential of *S. latissima* in the North Atlantic. We have not attempted to quantify possible enhancement in carbon sequestration rates or changes in the air/sea $CO_2$ flux. To do so would require a coupled physics/biogeochemistry/kelp model including seawater chemistry and a representation of intentional or natural sinking of the kelp biomass. Efforts to develop and test models of this type are needed to evaluate the strategy of growing kelp for the purpose of removing excess carbon dioxide from the ocean and atmosphere.

### 4.0.1 Permission to Reuse and Copyright

Figures, tables, and images will be published under a Creative Commons CC-BY licence and permission must be obtained for use of copyrighted material from other sources (including re-published/adapted/modified/partial figures and images from the internet). It is the responsibility of the authors to acquire the licenses, to follow any citation instructions requested by third-party rights holders, and cover any supplementary charges.

## 5 ADDITIONAL REQUIREMENTS

For additional requirements for specific article types and further information please refer to Author Guidelines.

## CONFLICT OF INTEREST STATEMENT

The authors declare that the research was conducted in the absence of any commercial or financial relationships that could be construed as a potential conflict of interest.

## AUTHOR CONTRIBUTIONS

JRT conceived and supervised the project. J S-W wrote the model code, ran the simulations and produced the figures. J S-W and JRT wrote the paper.

## FUNDING

J S-W was funded through the Undergraduate Summer Research Placement scheme from St. John's College, Cambridge.

## ACKNOWLEDGMENTS

The authors are grateful to the Centre for Climate Repair at Cambridge for stimulating conversations and encouraging this work. The authors also thank the team at Running Tide, Marty Odlin, Max Chalfin, Margaux Filippi, Olivia Alcabes, and Raj Saha, for helpful discussions and comments.

This study has been conducted using data from E.U. Copernicus Marine Service Information, and NASA's Joint Polar Satellite System and Moderate-resolution Imaging Spectroradiometer.

## SUPPLEMENTAL DATA

Supplementary Material should be uploaded separately on submission, if there are Supplementary Figures, please include the caption in the same file as the figure. LaTeX Supplementary Material templates can be found in the Frontiers LaTeX folder.

## DATA AVAILABILITY STATEMENT

The version of the model used in this paper is available at https://github.com/jagoosw/Kelp.jl/releases/tag/v1.0 and Zenode (**?**). The code used to preprocess the forcing data, run the model, and post process results is available at [github tag of paper repo] and Zenode **?**.

## REFERENCES

Ahn, O., Petrell, R. J., and Harrison, P. J. (1998). Ammonium and nitrate uptake by laminaria saccharina and nereocystis luetkeana originating from a salmon sea cage farm. *Journal of Applied Phycology* 10, 333–340

Aumont, O., Ethé, C., Tagliabue, A., Bopp, L., and Gehlen, M. (2015). Pisces-v2: an ocean biogeochemical model for carbon and ecosystem studies. *Geoscientific Model Development* 8, 2465–2513. doi:10.5194/gmd-8-2465-2015

Bartsch, I., Wiencke, C., Bischof, K., Buchholz, C. M., Buck, B. H., Eggert, A., et al. (2008). The genus laminaria sensu lato: recent insights and developments. *European journal of phycology* 43, 1–86

Bolton, J. J. and Lüning, K. (1982). Optimal growth and maximal survival temperatures of atlantic laminaria species (phaeophyta) in culture. *Marine Biology* 66, 89–94. doi:10.1007/BF00397259

Breeman, A. M. (1988). Relative importance of temperature and other factors in determining geographic boundaries of seaweeds: Experimental and phenological evidence. *Helgoländer Meeresuntersuchungen* 42, 199–241. doi:10.1007/BF02366043

Broch, O. J., Alver, M. O., Bekkby, T., Gundersen, H., Forbord, S., Handå, A., et al. (2019). The kelp cultivation potential in coastal and offshore regions of norway. *Frontiers in Marine Science* 5, 529

Broch, O. J., Ellingsen, I., Forbord, S., Wang, X., Volent, Z., Alver, M., et al. (2013). Modelling the cultivation and bioremediation potential of the kelp saccharina latissima in close proximity to an exposed salmon farm in norway. *Aquaculture Environment Interactions* 4, 187–206. doi:10.3354/aei00080

Broch, O. J. and Slagstad, D. (2012). Modelling seasonal growth and composition of the kelp saccharina latissima. *Journal of Applied Phycology* 24, 759–776. doi:10.1007/s10811-011-9695-y

Canadell, J., Monteiro, P., Costa, M., Cotrim da Cunha, L., Cox, P., Eliseev, A., et al. (2021). *Global Carbon and other Biogeochemical Cycles and Feedbacks. In Climate Change 2021: The Physical Science Basis. Contribution of Working Group I to the Sixth Assessment Report of the Intergovernmental Panel on Climate Change [Masson- Delmotte, V., P. Zhai, A. Pirani, S.L. Connors, C. Péan, S. Berger,*

*N. Caud, Y. Chen, L. Goldfarb, M.I. Gomis, M. Huang, K. Leitzell, E. Lonnoy, J.B.R. Matthews, T.K. Maycock, T. Waterfield, O. Yelekçi, R. Yu, and B. Zhou (eds.)]* (Cambridge University Press. In Press)

[Dataset] E.U. Copernicus Marine Service Information (2021a). Global ocean 1/12° physics analysis and forecast updated daily. Accessed between 15/07/2021 & 15/09/2021. Available at: https://resources.marine.copernicus.eu/product-detail/GLOBAL_ANALYSIS_FORECAST_PHY_001_024

[Dataset] E.U. Copernicus Marine Service Information (2021b). Global ocean biogeochemistry analysis and forecast. Accessed between 15/07/2021 & 15/09/2021. Available at: https://resources.marine.copernicus.eu/product-detail/GLOBAL_ANALYSIS_FORECAST_BIO_001_028

[Dataset] E.U. Copernicus Marine Service Information (2021c). Global ocean biogeochemistry hindcast. Accessed between 15/07/2021 & 15/09/2021. Available at: https://resources.marine.copernicus.eu/productdetail/GLOBAL_REANALYSIS_BIO_001_029

[Dataset] E.U. Copernicus Marine Service Information (2021d). Global ocean ensemble physics reanalysis. Accessed between 15/07/2021 & 15/09/2021. Available at: https://resources.marine.copernicus.eu/productdetail/GLOBAL_REANALYSIS_PHY_001_031/

Fossberg, J., Forbord, S., Broch, O. J., Malzahn, A. M., Jansen, H., Handå, A., et al. (2018). The potential for upscaling kelp (saccharina latissima) cultivation in salmon-driven integrated multi-trophic aquaculture (imta). *Frontiers in Marine Science* 5, 418. doi:10.3389/fmars.2018.00418

Gerard, V. A. and Du Bois, K. R. (1988). Temperature ecotypes near the southern boundary of the kelp laminaria saccharina. *Marine Biology* 97, 575–580. doi:10.1007/BF00391054

Jevne, L. S., Forbord, S., and Olsen, Y. (2020). The effect of nutrient availability and light conditions on the growth and intracellular nitrogen components of land-based cultivated saccharina latissima (phaeophyta). *Frontiers in Marine Science* 7, 914. doi:10.3389/fmars.2020.557460

Krause-Jensen, D., Sejr, M. K., Bruhn, A., Rasmussen, M. B., Christensen, P. B., Hansen, J. L. S., et al. (2019). Deep penetration of kelps offshore along the west coast of greenland. *Frontiers in Marine Science* 6, 375. doi:10.3389/fmars.2019.00375

Kwiatkowski, L., Torres, O., Bopp, L., Aumont, O., Chamberlain, M., Christian, J. R., et al. (2020). Twenty-first century ocean warming, acidification, deoxygenation, and upper-ocean nutrient and primary production decline from cmip6 model projections. *Biogeosciences* 17, 3439–3470. doi:10.5194/bg-17-3439-2020

Lee, J.-Y., Marotzke, J., Bala, G., Cao, L., Corti, S., Dunne, J., et al. (2021). *Future Global Climate: Scenario-Based Projections and Near-Term Information. In Climate Change 2021: The Physical Science Basis. Contribution of Working Group I to the Sixth Assessment Report of the Intergovernmental Panel on Climate Change [Masson- Delmotte, V., P. Zhai, A. Pirani, S.L. Connors, C. Péan, S. Berger, N. Caud, Y. Chen, L. Goldfarb, M.I. Gomis, M. Huang, K. Leitzell, E. Lonnoy, J.B.R. Matthews, T.K. Maycock, T. Waterfield, O. Yelekçi, R. Yu, and B. Zhou (eds.)]* (Cambridge University Press. In Press)

Louanchi, F. and Najjar, R. G. (2001). Annual cycles of nutrients and oxygen in the upper layers of the north atlantic ocean. *Deep Sea Research Part II: Topical Studies in Oceanography* 48, 2155–2171. doi:https://doi.org/10.1016/S0967-0645(00)00185-5. JGOFS Research in the North Atlantic Ocean: A Decade of Research, Synthesis and modelling

Lubsch, A. and Timmermans, K. R. (2019). Uptake kinetics and storage capacity of dissolved inorganic phosphorus and corresponding dissolved inorganic nitrate uptake in saccharina latissima and laminaria digitata (phaeophyceae). *Journal of Phycology* 55, 637–650. doi:https://doi.org/10.1111/jpy.12844

Luning, K. (1979). Growth strategies of three laminaria species (phaeophyceae) inhabiting different depth zones in the sublittoral region of helgoland (north sea). *Marine Ecology Progress Series* 1, 195–207. doi:10.3354/meps001195

Molen, J. v. d., Ruardij, P., Mooney, K., Kerrison, P., O'Connor, N. E., Gorman, E., et al. (2018). Modelling potential production of macroalgae farms in uk and dutch coastal waters. *Biogeosciences* 15, 1123–1147

Morel, A. (1988). Optical modeling of the upper ocean in relation to its biogenous matter content (case i waters). *Journal of Geophysical Research: Oceans* 93, 10749–10768. doi:https://doi.org/10.1029/JC093iC09p10749

Morel, A. and Maritorena, S. (2001). Bio-optical properties of oceanic waters: A reappraisal. *Journal of Geophysical Research: Oceans* 106, 7163–7180. doi:https://doi.org/10.1029/2000JC000319

[Dataset] NASA Goddard Space Flight Center, Ocean Ecology Laboratory, Ocean Biology Processing Group (2021a). Moderate-resolution imaging spectroradiometer (modis) aqua photosynthetically available radiation. doi:https://www.doi.org/10.5067/AQUA/MODIS/L3B/PAR/2018. Accessed on 22/07/2021

[Dataset] NASA Goddard Space Flight Center, Ocean Ecology Laboratory, Ocean Biology Processing Group (2021b). Visible and infrared imager/radiometer suite (viirs) photosynthetically available radiation data. doi:https://www.doi.org/10.5067/JPSS1/VIIRS/L3B/PAR/2018. Accessed on 22/07/2021

Nielsen, M. M., Krause-Jensen, D., Olesen, B., Thinggaard, R., Christensen, P. B., and Bruhn, A. (2014). Growth dynamics of saccharina latissima (laminariales, phaeophyceae) in aarhus bay, denmark, and along the species' distribution range. *Marine Biology* 161, 2011–2022. doi:10.1007/s00227-014-2482-y

Nielsen, M. M., Manns, D., D'Este, M., Krause-Jensen, D., Rasmussen, M. B., Larsen, M. M., et al. (2016). Variation in biochemical composition of saccharina latissima and laminaria digitata along an estuarine salinity gradient in inner danish waters. *Algal Research* 13, 235–245. doi:https://doi.org/10.1016/j.algal.2015.12.003

Redfield, A. C. (1934). *On the proportions of organic derivatives in sea water and their relation to the composition of plankton*, vol. 1 (University Press of Liverpool Liverpool)

Rogelj, J., Popp, A., Calvin, K. V., Luderer, G., Emmerling, J., Gernaat, D., et al. (2018). Scenarios towards limiting global mean temperature increase below 1.5 °c. *Nature Climate Change* 8, 325–332. doi:10.1038/s41558-018-0091-3

[Dataset] Running Tide (2021). Stripe carbon removal proposal: https://github.com/stripe/carbon-removal-source-materials/find/master

Sanders, R., Henson, S. A., Koski, M., De La Rocha, C. L., Painter, S. C., Poulton, A. J., et al. (2014). The biological carbon pump in the north atlantic. *Progress in Oceanography* 129, 200–218. doi:https://doi.org/10.1016/j.pocean.2014.05.005. North Atlantic Ecosystems, the role of climate and anthropogenic forcing on their structure and function

Sjøtun, K. (1993). Seasonal lamina growth in two age groups of laminaria saccharina (l.) lamour. in western norway: 36, 433–442. doi:doi:10.1515/botm.1993.36.5.433

[Dataset] Strong-Wright, J. (2021). SugarKelp.jl. doi:10.5281/zenodo.5554954

van Den Hoek, C. (1982). The distribution of benthic marine algae in relation to the temperature regulation of their life histories. *Biological Journal of the Linnean Society* 18, 81–144. doi:10.1111/j.1095-8312.1982.tb02035.x

Venolia, C. T., Lavaud, R., Green-Gavrielidis, L. A., Thornber, C., and Humphries, A. T. (2020). Modeling the growth of sugar kelp (saccharina latissima) in aquaculture systems using dynamic energy budget theory. *Ecological Modelling* 430, 109151

Whiting, J. M., Wang, T., Yang, Z., Huesemann, M. H., Wolfram, P. J., Mumford, T. F., et al. (2020). Simulating the trajectory and biomass growth of free-floating macroalgal cultivation platforms along the us west coast. *Journal of Marine Science and Engineering* 8, 938

Yang, B., Fox, J., Behrenfeld, M. J., Boss, E. S., Haëntjens, N., Halsey, K. H., et al. (2021). In situ estimates of net primary production in the western north atlantic with argo profiling floats. *Journal of Geophysical Research: Biogeosciences* 126, e2020JG006116